

Reliable Information Transmission along QCA Wires in the Presence of Non-Adiabatic Transitions

Daniel Brox: EECE, University of British Columbia

April 14, 2017

Abstract

Quantum dot cellular automata (QCA) computing schemes use arrays of quantum dots as computational devices. Typically, these operate ideally by maintaining arrays in their ground state to ensure correct computational output. For large QCA circuits, thermal fluctuations make this impossible, so adiabatic clocking has been proposed as a means of dividing large circuit computations into subcircuit computations that are more reliable. In this report, it is shown that wires and inverters can transmit information correctly via their excited states just as well as their ground states. A characteristic example of a 4 cell wire is simulated, and a theoretical derivation of this result is given. When, non-nearest neighbor interactions are included in the Hamiltonian, this result still holds true. On the other hand, QCA majority gates and more complex circuits give incorrect results when operated in excited states. These results suggest that gates of reliable QCA circuits should be contained in smaller clocking zones, while wires relaying information can be contained in larger clocking zones.

Introduction

In the drive to continue to increase computing power, methods of computing based on quantum-dot cellular automata (QCA) have been proposed as an alternative to conventional computing [1]. Rather than switching between states of current flow, these methods work by manipulating electronic configurations within atomic scale physical systems such as groups of atoms or quantum dots, offering the potential of speeding up and reducing the size of digital circuits [2]. Essential to operation of QCA circuits is the switching of input cell states so that new computations can be performed by the same circuit. This switching must be performed with care, since it is desirable that QCA circuits remain in their lowest energy state throughout operation to ensure the correct electronic states of output cells. As a means of achieving this, adiabatic clocking schemes have been proposed whereby tunneling between quantum states of all non-input QCA cells is enabled while the polarization of the input cells is switched, and tunneling is disabled when switching is completed. In so doing, the adiabatic theorem of quantum mechanics guarantees that if an energy gap is maintained between the ground and excited states of the entire QCA circuit and switching is slow enough, the circuit will stay in its ground state with high probability through switching and the correct computation will be performed [3].

However, there are still theoretical questions to be answered regarding how well we should expect this technique to work for a particular physical implementation when the environment of a circuit affects its operation. For instance, a silicon dangling bond QCA circuit will consist of cells fabricated on the surface of a silicon wafer interacting with thermal vibrations in the silicon lattice that can potentially flip the states of its cell states via phonon emission / absorption [4]. This is indicated in Fig. 1, where the third cell of a four cell wire has switched its electronic configuration by absorbing a phonon.

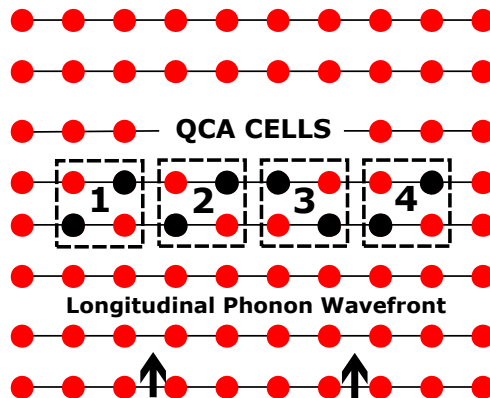


Fig. 1 State flipping of a silicon dangling bond qubit due to interaction with longitudinal phonons in a silicon lattice. Localized electrons are shown as black dots and silicon atoms as red dots. In this image, qubit 3 has flipped its electronic state by absorbing a phonon.

In general, excitation of a QCA circuit out of its ground state by its environment can cause computation to give an incorrect answer. This event becomes more and more likely as the number of cells in the QCA circuit increases, so it has been suggested that dividing a QCA circuit into separately clocked zones with small numbers of cells will allow each zone to perform with high fidelity independently of the others. If this is true, the probability of error occurring in any particular zone circuit during its computation cycle can be made small by sufficiently reducing the number of cells in the zone and ensuring the energy gap between the ground state and first excited state of each clocking zone circuit is large compared to the thermal energy scale $k_B T$. Of course, in a sufficiently

large QCA circuit, a fraction of the zone circuits will not be in their ground states, and we cannot assume that they will compute correctly as a consequence of the adiabatic theorem. However, from a computational perspective, we only care about whether or not a circuit gives the correct output for a given set of computation inputs, and not about what quantum state it starts out in. Therefore, the question arises as to whether or not excited states of zone circuits can be utilized for computation, as if this is possible, the reliability of the circuit is enhanced and the amount of error correction in the overall circuit may be reduced [5]. Initially, one might expect that the answer to this question is no, since non-adiabatic transitions between excited states of an adiabatically clocked circuit may randomize its output. However, for the case of a QCA wire, the structure of the Hamiltonian describing its quantum evolution enables information to be transmitted reliably via excited states [6]. This finding has implications for QCA circuit design, since it suggests that a lower density of clocking zones may be used to relay information between different regions of a circuit where a higher density of gate containing zones should be used to perform computation.

QCA Wire

A simple simulation of a 4 cell QCA wire demonstrates the phenomenon of interest. Fig. 2 shows two possible wire starting states from which we'd like to switch the input of the wire adiabatically to transmit information:

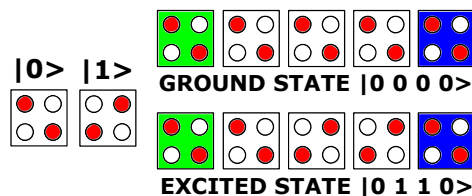


Fig. 2 Schematic of ground and excited states of a four cell QCA wire.

In these wire states, each cell exists in a definite $|0\rangle$ or $|1\rangle$ state and the overall wire state is the tensor product of 4 such states. The green input cell state is treated as a continuously varying polarization $P_{in}(t)$. This is indicated in the QCA wire Hamiltonian:

$$\begin{aligned}
 H_{wire}(t) = & -\frac{E_k}{2}P_{in}(t)\sigma_z^1 + \frac{E_k}{2}\gamma(t)(\sigma_x^1 + \sigma_x^2 + \sigma_x^3 + \sigma_x^4) \\
 & -\frac{E_k}{2}(\sigma_z^1\sigma_z^2 + \sigma_z^2\sigma_z^3 + \sigma_z^3\sigma_z^4),
 \end{aligned} \tag{1}$$

where E_k is the kink energy associated with neighboring cells having different polarizations (ie. $|0\rangle$ and $|1\rangle$ states), and $\gamma(t)$ is the adiabatic clocking signal that enables / disables cell tunneling. More specifically, when $|\gamma(t)| \approx 1$, cell tunneling is enabled and the cell state is “unlatched”, and when $|\gamma(t)| \approx 0$, cell tunneling is disabled and the cell state is “latched”. Note that because there is only one adiabatic clocking signal $\gamma(t)$ in the Hamiltonian, we are modeling the wire as a singly clocked zone.

The operators σ_z^i and σ_x^i in the Hamiltonian are Pauli matrices [7] acting on the i^{th} cell, which is mathematically equivalent to a qubit in the two state approximation. The σ_z^i operators in the Hamiltonian are referred to as polarization operators, and defined so that the cell states $|0\rangle$ and $|1\rangle$ are eigenvectors with eigenvalues -1 and 1. For example:

$$\sigma_z^1|0110\rangle = -|0110\rangle, \quad (2)$$

$$\sigma_z^2|0110\rangle = |0110\rangle, \quad (3)$$

$$\sigma_z^3|0110\rangle = |0110\rangle, \quad (4)$$

$$\sigma_z^4|0110\rangle = -|0110\rangle. \quad (5)$$

Simulation of adiabatic switching is achieved by solving the time dependent Schrodinger equation:

$$i\hbar \frac{\partial}{\partial t} |\Psi(t)\rangle = H_{wire}(t) |\Psi(t)\rangle, \quad (6)$$

from $t = 0$ to some final time $t = t_f$ with some choice of functions $P_{in}(t)$ and $\gamma(t)$ such that $P_{in}(t_f) = -1$, $\gamma(t_f) = 0$, and the gap energy between the wire ground and first excited state is nonzero throughout the switching interval. For this purpose, we can set:

$$P_{in}(t) = \cos(\pi t/t_f), \quad (7)$$

$$\gamma(t) = \gamma_{max} \cdot \sin(\pi t/t_f). \quad (8)$$

We then have two remaining parameters t_f and γ_{max} to choose. Since γ_{max} will be chosen to maintain the gap energy between the ground and first excited state close to the kink energy E_k , it follows that we should choose $t_f \gg \hbar/E_k$ to avoid non-adiabatic transitions from the ground state to the first excited state. Selecting $t_f = 30\hbar/E_k$ to satisfy this condition, we can plot the instantaneous energy spectrum (first 4 levels) of the QCA wire for each time $t \in [0, t_f]$ for different values of γ_{max} to determine a suitable value. Fig. 3 shows three such plots for $\gamma_{max} = 0.1, 0.5$, and 2.0 , with energy in units of E_k and time in units of \hbar/E_k .

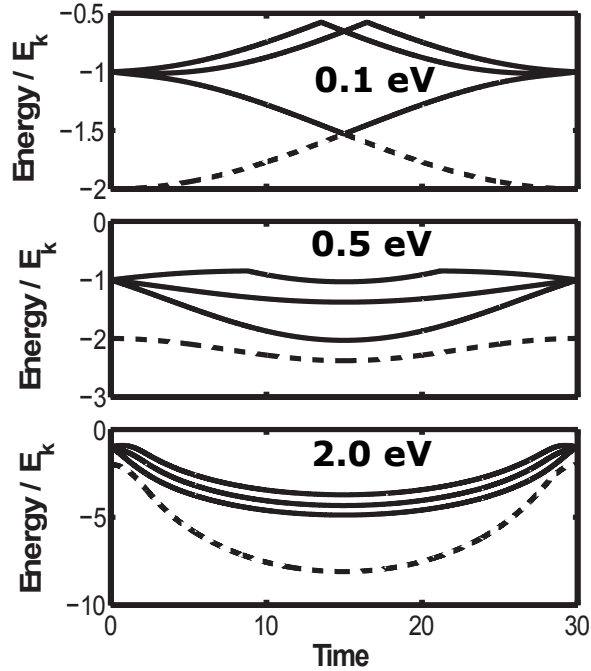


Fig. 3 Four cell QCA wire energy spectra throughout adiabatic clocking for clocking signals with different maxima.

When $\gamma_{max} = 0.1$ there is a level crossing between the ground state (dashed) and first excited state (solid) which enhances non-adiabatic transitions, so we adopt $\gamma_{max} = 0.5$ as a practical value. We can then solve the time dependent Schrodinger equation for $|\Psi(t_f)\rangle$ starting from the two different initial states $|0000\rangle$ and $|0110\rangle$ and evaluate the transition probabilities to the various possible wire final states. Starting from the state $|0000\rangle$, the switched wire ends up in its new ground state $|1111\rangle$ with probability 0.9858. Furthermore, summing over transition probabilities, the likelihood that the last cell in the wire is in the $|1\rangle$ state after switching is 0.9868. On the other hand, starting from the $|0110\rangle$ excited state, several non-adiabatic transitions to other excited states occur. However, summing over transition probabilities to states with last cell polarized in the $|1\rangle$ state, we obtain 0.9868 again. This result is summarized in Fig. 4.

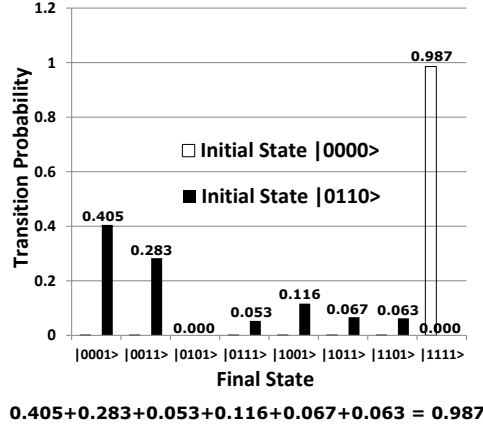


Fig. 4 Transition probabilities to various wire states with output polarization 1 after adiabatic switching is completed. The two shades represent different initial states. In both cases the total probability is the same.

This result generalizes to wires of arbitrary length, kink energies, choice of input polarization, and clocking functions. It also holds for singly-branched inverters of the form shown in Fig. 5. In the case of adiabatic switching, the number of kinks in the wire between initial and final wire states is conserved with high probability as in Fig. 4. This is not a consequence of adiabaticity alone, but is particular to the structure of the QCA wire Hamiltonian.

For more complex circuits such as the majority and doubly-branched inverter gates shown in Fig. 6, the result does not hold. In this figure, the ground and excited initial states of majority and inverter gates are indicated together with the expected polarizations of the output cell after the leftmost input cell is adiabatically switched from $|0\rangle$ to $|1\rangle$. When a switching time of $t_f = 30\hbar/E_k$ is used for the majority gate and a switching time of $t_f = 60\hbar/E_k$ is used for the inverter, the respective expected values of the output cell polarizations (ie. Pauli operator) after switching from the ground states are 0.9852 and 0.8569. Both these polarizations correspond to the desired $|1\rangle$ output state. However, flipping states of internal cells in the initial configuration of either circuit to generate excited states result in negative output polarizations after switching, corresponding to the undesired $|0\rangle$ output state. It follows that excited states of these circuits cannot be reliably used for computation.

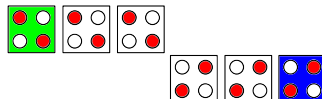


Fig. 5 Singly-branched inverter circuit with similar QCA Hamiltonian structure as a wire.

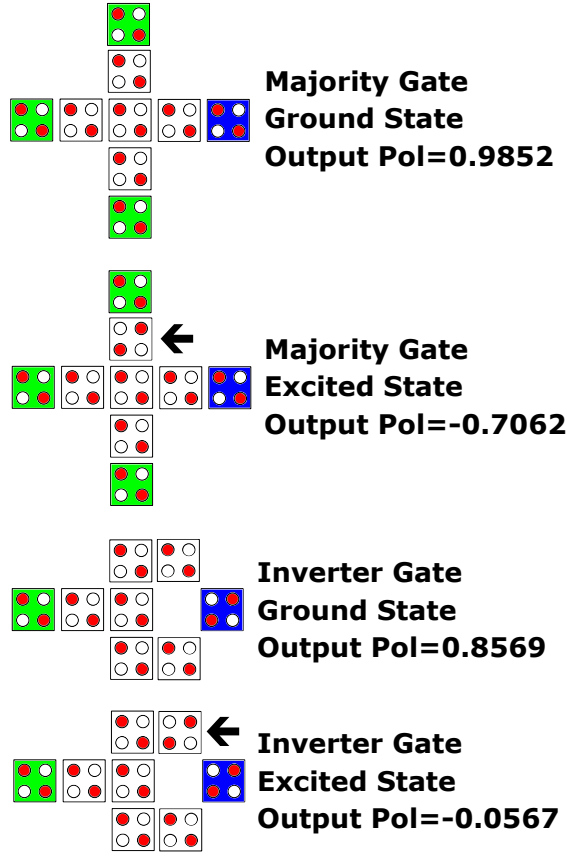


Fig. 6 Schematics of QCA majority and inverter gate circuits.

Derivation

In general, for an $N + 1$ cell wire with a single input cell and general clocking, we can write the wire Hamiltonian as:

$$\begin{aligned}
 H_{wire}(t) = & -\frac{E_k}{2}P_{in}(t)\sigma_z^1 + \frac{E_k}{2}\sum_{i=1}^N\gamma^i(t)\sigma_x^i \\
 & -\frac{E_k}{2}\sum_{i=1}^{N-1}\sigma_z^i\sigma_z^{i+1}.
 \end{aligned} \tag{9}$$

Information is transmitted along the wire by adjusting the input polarization $P_{in}(t)$ and clocking signals $\gamma^i(t)$. The input polarization affects the leftmost cell 1, and the wire output is the N^{th} cell. The coherent evolution of the wire is governed by the time-dependent Schrodinger equation, or equivalently, the Von Neumann equation [8]:

$$\dot{\rho} = -\frac{i}{\hbar}[H_{wire}(t), \rho], \tag{10}$$

where ρ is the density matrix of the wire describing a pure state. The expected polarization of the wire output is given by:

$$P_{out}(t) = Tr(\sigma_z^N \rho). \tag{11}$$

This output polarization can be switched adiabatically by slowly varying the input polarization and clocking signals. We now prove that $P_{out}(t_f)$ only depends on the initial expected values of a particular set of operators, so that any state with the same expectation values at $t = 0$ will evolve into a state with the same output polarization.

To do this, for reasons that will become clear, rename:

$$Z_0(t) = P_{out}(t) = Tr(\sigma_z^N \rho), \quad (12)$$

so that:

$$\begin{aligned} \dot{Z}_0(t) &= Tr(\sigma_z^N \dot{\rho}), \\ &= -\frac{i}{\hbar} Tr(\sigma_z^N [H_{wire}(t), \rho]), \\ &= -\frac{i}{\hbar} Tr([\sigma_z^N, H_{wire}(t)] \rho), \\ &= -\frac{i}{\hbar} Tr((E_k \gamma^N(t) i \sigma_y^N) \rho), \\ &= \frac{E_k}{\hbar} \gamma^N(t) Tr(\sigma_y^N \rho). \end{aligned} \quad (13)$$

Similarly, letting $Y_0(t) = Tr(\sigma_y^N \rho)$:

$$\begin{aligned} \dot{Y}_0(t) &= Tr(\sigma_y^N \dot{\rho}), \\ &= -\frac{i}{\hbar} Tr([\sigma_y^N, H_{wire}(t)] \rho), \\ &= -\frac{i}{\hbar} Tr((-E_k \gamma^N(t) i \sigma_z^N - E_k \sigma_z^{N-1} i \sigma_x^N) \rho), \\ &= -\frac{E_k}{\hbar} \gamma^N(t) Tr(\sigma_z^N \rho) - \frac{E_k}{\hbar} Tr(\sigma_z^{N-1} \sigma_x^N \rho), \end{aligned} \quad (14)$$

and more generally, defining:

$$Z_i(t) = Tr(\sigma_z^{N-i} \sigma_x^{N-i+1} \dots \sigma_x^N \rho), \quad (15)$$

$$Y_i(t) = Tr(\sigma_y^{N-i} \sigma_x^{N-i+1} \dots \sigma_x^N \rho), \quad (16)$$

we find:

$$\dot{Z}_i(t) = \frac{E_k}{\hbar} \gamma^{N-i}(t) Y_i(t) + \frac{E_k}{\hbar} Y_{i-1}(t), \quad (17)$$

$$\dot{Y}_i(t) = -\frac{E_k}{\hbar} \gamma(t) Z_i(t) - \frac{E_k}{\hbar} Z_{i+1}(t). \quad (18)$$

These equations hold true except for $Y_{N-1}(t)$, where:

$$\dot{Y}_{N-1}(t) = \frac{E_k}{\hbar} P_{in}(t) Z_N(t), \quad (19)$$

$$Z_N(t) = Tr(\sigma_x^1 \sigma_x^2 \dots \sigma_x^N \rho), \quad (20)$$

and:

$$\dot{Z}_N(t) = -\frac{E_k}{\hbar} P_{in}(t) Y_{N-1}(t). \quad (21)$$

Since these equations form a system of linear ordinary differential equations, it follows that all the expected values $\{Z_i(t), Y_i(t)\}$ at any given time only depend on their values at $t = 0$. In particular, if we start out in a state where the output polarization is latched: $\gamma^N(0) = 0$, and we assume the polarization has a definite value $P_{out}(0) = \pm 1$, it follows $Z_0(0) = \pm 1$, and all other initial values are 0. All such states, regardless of whether or not they are the ground state, evolve with the same output polarization. Note that this derivation does not depend on the uniformity or sign of the kink energy E_k between nearest neighbors, and thus works equally well for singly-branched inverters.

Non-Nearest Neighbor Interactions

Given that the derivation in the previous section is particular to the wire Hamiltonian, and this wire Hamiltonian is an approximation that ignores effects such as non-nearest neighbor interactions, it is important to consider the effects of these interactions on information transmission. Therefore, a modification of the wire Hamiltonian taking into consideration next-to-nearest neighbor interactions is made as shown below for the four cell wire:

$$H_{total}(t) = H_{wire}(t) + H_I(t), \quad (22)$$

$$H_{wire}(t) = -\frac{E_k}{2} P_{in}(t) \sigma_z^1 + \frac{E_k}{2} \gamma(t) (\sigma_x^i + \sigma_x^i + \sigma_x^i + \sigma_x^i) - \frac{E_k}{2} (\sigma_z^1 \sigma_z^2 + \sigma_z^2 \sigma_z^3 + \sigma_z^3 \sigma_z^4), \quad (23)$$

$$H_I(t) = -\frac{E_k}{64} (\sigma_z^1 \sigma_z^3 + \sigma_z^2 \sigma_z^4). \quad (24)$$

In this Hamiltonian, the kink energy between next-to-nearest neighbor cells is lower by a factor of $2^{-5} = 1/32$ over the neighboring interaction due to the quadrupole-quadrupole interaction between QCA cells. Using the corresponding Hamiltonian for 6 and 7 cell wires, the following table shows the computed output cell polarizations for $60\hbar/E_k$ adiabatic switching cycles starting from different initial wire states next to their corresponding unperturbed values:

TABLE I: Expected output cell polarization after adiabatic switching from different initial wire states.

Initial Wire State	$H_I(t) = 0$	$H_I(t) \neq 0$
[000000] - 6 cell	0.9932	0.9572
[000010] - 6 cell	0.9932	0.9798
[000100] - 6 cell	0.9932	0.9854
[010000] - 6 cell	0.9932	0.9794
[010100] - 6 cell	0.9932	0.9949
[101010] - 6 cell	0.9932	0.9966
[0000000] - 7 cell	0.9784	0.8795
[0011000] - 7 cell	0.9784	0.9492
[1001000] - 7 cell	0.9784	0.9797
[1101100] - 7 cell	0.9784	0.9753

This data shows that with non-nearest neighbor interactions, the ground state and excited state final cell polarizations after switching are no longer equivalent, but are small perturbations of the identical polarization obtained in the absence of such interactions. Furthermore, in all cases simulated, including all excited states of a 6 cell wire, the excited state performs better than the ground state. Fig. 7 shows a plot of the difference between the cell 6 output polarizations with next-to-nearest neighbor interaction and without vs time (units \hbar/E_k) for the ground state and two excited states:

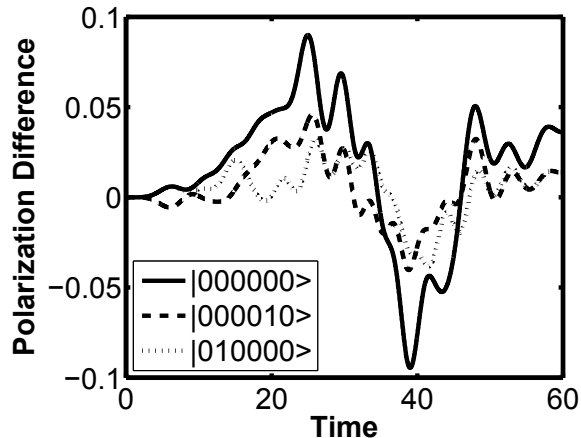


Fig. 7 Difference between cell 6 output polarizations of wires with and without next-to-nearest neighbors for starting from the ground state and two excited states.

In this figure, the fact that the ground state polarization difference at the $t = 60\hbar/E_k$ end of switching is greater than the excited state polarization difference accounts for the better performance of the excited states. It also appears that the excited state polarization differences roughly mimic the ground state polarization differences but are scaled down.

To get a sense of why this is true, we can write the density matrix ρ which evolves under the action of the Hamiltonian H_{total} as the sum of two pieces:

$$\rho(t) = \rho_{wire}(t) + \rho_I(t), \quad (25)$$

where:

$$\dot{\rho}_{wire}(t) = -\frac{i}{\hbar} [H_{wire}(t), \rho_{wire}(t)], \quad (26)$$

$$\rho_{wire}(0) = \rho(0). \quad (27)$$

From this it follows from the Von Neumann equation for ρ that:

$$\dot{\rho}_{wire} + \dot{\rho}_I = -\frac{i}{\hbar} [H_{wire} + H_I, \rho_{wire} + \rho_I], \quad (28)$$

$$\dot{\rho}_I = -\frac{i}{\hbar} [H_{wire} + H_I, \rho_I] - \frac{i}{\hbar} [H_I, \rho_{wire}], \quad (29)$$

$$\rho_I(0) = 0, \quad (30)$$

and by similar manipulations to those of the previous section:

$$\frac{d}{dt}Tr(\sigma_z^N \rho_I) = \frac{E_k}{\hbar}Tr(\sigma_y^N \rho_I)\gamma^N(t), \quad (31)$$

$$Tr(\sigma_z^N \rho_I(0)) = 0. \quad (32)$$

This equation is of interest because $Tr(\sigma_z^N \rho_I)$ is the change to the expected polarization of the N^{th} cell in the wire induced by non-nearest neighbor interactions. Its initial value is zero, and its rate of change is proportional to the y-polarization of the cell. If we assume that ρ_I is negligible compared to ρ_{wire} , we can further approximate:

$$\frac{d}{dt}Tr(\sigma_y^N \rho_I) \approx -\frac{E_k}{\hbar}Tr(\sigma_z^{N-2} \sigma_x^N \rho_{wire}(t)), \quad (33)$$

and the function of time on the right depends on the initial state of the wire. It appears this function is highly oscillatory for excited states while not so for the ground state, so $Tr(\sigma_y^N \rho_I)$ is correspondingly smaller for excited states, as is the final output polarization $Tr(\sigma_z^N \rho_I)$. Of course, this is only heuristic argument, and a more rigorous theoretical derivation remains outstanding.

Conclusions

Simulation of QCA wires suggests that initial occupation of the wire ground state is not necessary for reliable information transmission, despite the occurrence of non-adiabatic transitions in the case where the initial state is excited. In the case where non-nearest neighbor interactions are neglected from the wire Hamiltonian, it is derived that there is identical behavior of information transmission along QCA wires and singly-branched inverters occupying their ground or excited states. On the other hand, other simple circuits such as majority and double-branched inverter gates do not share this property. Therefore, in a QCA circuit that has been divided into separate individually clocked zones, this suggests that wires used to relay information around the circuit are still functional after environmental excitation of their quantum state, while gates are not. This information is of relevance in designing QCA circuits with appropriate error correction, as it suggests gates performing computations should be contained in smaller clocking zones than wires relaying information for optimized circuit performance.

Acknowledgment

This work was supported by an NSERC Engage grant in partnership with Quantum Silicon Inc.

References

- [1] C. Lent, P. Tougdaw, "A device architecture for computing with quantum dots", *Proc. IEEE*, vol. 85, no. 4, pp. 541 - 557, 1997.
- [2] J. Timler, C. Lent, "Power gain and dissipation in quantum-dot cellular automata", *Journal of Applied Physics*, vol. 91, no. 2, pp. 823 - 831, 2002.
- [3] T. Kato, "On the adiabatic theorem of quantum mechanics". *Journal of the Physical Society of Japan*, vol. 5, no. 6, pp. 435 - 439, 1950.
- [4] L. Livadaru, P. Xue, Z. Shaterzadeh-Yazdi, G. DiLabio, J. Mutus, J. Pitters, B. Sanders, R. Wolkow, "Dangling-bond charge qubit on a silicon surface", *New Journal of Physics*, vol. 12, no. 8,

083018, 2010.

- [5] S. Srivastava, S. Bhanja, "Hierarchical probabilistic macromodeling for QCA circuits." *IEEE Transactions on Computers*, vol. 56, no. 2, pp. 174 - 190, 2007.
- [6] C. Zener, "Non-adiabatic crossing of energy levels", *Proceedings of the Royal Society of London. Series A, Containing Papers of a Mathematical and Physical Character*, vol. 137, no. 833, pp. 696 - 70, 1932.
- [7] F. Karim, A. Navabi, K. Walus, A. Ivanov "Quantum mechanical simulation of QCA with a reduced Hamiltonian model", *Proceedings of the 8th IEEE Conference on Nanotechnology, 2008*.
- [8] G. Mahler, and A. Volker, *Quantum networks, Dynamics of open nanostructures*, Springer-Verlag Berlin Heidelberg (1998).